Original Article

MOLECULAR METABOLISM

Selective adipocyte loss of Angiopoietin-2 prompts female-specific obesity and metabolic syndrome

Bin Ni [1,2], Shanshan Chen [1,3], Kathleen A. Ryan [4], Michael L. Maitland [5,6], Jared S. Farrar [7], Martin Witzenrath [8,9], Birgitt Gubier [8], Cindy Serdjebi [10], Karine Bertotti [10], Rui Wang [11], Fadi N. Salloum [11], Luigi Marino [1], Braxton D. Mitchell [4,12], Francesco S. Celi [1,*]

ABSTRACT

Thermogenic fat differentiation and function can be promoted through multiple pathways, resulting in a common cell phenotype characterized by the expression of Uncoupling Protein-1 and the ability to dissipate energy, but local and systemic stimuli are necessary to promote adequate thermogenic fat vascularization, which is a precondition for the transport of substrate and the dissipation of heat. Angiopoietin-2 is an important driver of vascularization, and its transcription is in part promoted by estrogen signaling. In this study we demonstrate that adipose tissue-specific knock out of Angiopoietin-2 causes a female-specific reduced thermogenic fat differentiation and function, resulting in obesity and impaired glucose tolerance with end-organ features consistent with metabolic syndrome. In humans, angiopoietin-2 levels are higher in females than in males, and are inversely correlated with adiposity and age more strongly in pre-menopause when compared to post-menopause. Collectively, these data indicate a novel and important role for estrogen-mediated Angiopoietin-2 adipose tissue production in the protection against calorie overload in females, and potentially in the development of postmenopausal weight gain.

Keywords ANGPT2; Ucp1; Brown fat; Estrogen; Obesity; Female

1. INTRODUCTION

Thermogenic fat (brown and beige adipose tissue-[AT]) has the unique ability of dissipating energy through the transcription and activity of Uncoupling Protein 1 (UCP-1) [1]. While its expansion results in resistance to obesity and its metabolic consequences, impairment promotes weight gain [2]. Aside from its role in non-shivering thermogenesis, thermogenic fat plays a pivotal role in the thermic effect of food, which is thought to be a short-loop response against calorie overload [3]. The plasticity of thermogenic fat, and in particular beige fat, allows for differentiation, expansion, and activation following different pathways, which result in a common adipocyte phenotype. The increased substrate utilization in turn promotes improvement in insulin sensitivity and resistance to end-organ damage resulting from calorie overload such as chronic inflammation, ectopic deposition of lipids, and cardiovascular dysfunction [4]. Irrespective of the stimulatory pathway, expansion of the capillary bed surrounding the adipocytes is a common feature of thermogenic fat, which allows for efficient delivery of substrate and dissipation of thermal energy, resulting in one of the most vascularized tissues of the organism [5]. The vascularization of thermogenic fat is driven by systemic and paracrine angiogenic factors [6], while endothelial cells and pericytes serve as a stem cell reservoir for supplying preadipocytes [7]. Reciprocally, adipocytes produce various angiogenic factors, including vascular endothelial growth factor (VEGF) and angiopoietin [8]. Enhanced angiogenesis promotes healthy thermogenic fat expansion, decreases inflammation, and minimizes fibrotic damage. Conversely, inadequate angiogenesis leads to adipose tissue hypoxia, enlarged adipocyte size, increased inflammation, and fibrosis [9]. Increased angiogenesis during early adipose tissue expansion could thus improve metabolic response to sustained positive energy balance, minimizing the negative systemic consequences of obesity [10].

Most preclinical models of obesity have been conducted in male mice because they are extremely sensitive to high-fat diet (HFD)-induced obesity and its metabolic consequences [11,12], while female mice are protected against HFD [13]. Upon HFD feeding, perigonadal fat in female

[1]Department of Internal Medicine, Division of Endocrinology, Diabetes and Metabolism, Virginia Commonwealth University School of Medicine, Richmond, VA, USA [2]Central Virginia VA Health Care System (CVHCS)/McGuire VA Medical Center, Richmond, VA, USA [3]Department of Biostatistics, Virginia Commonwealth University School of Medicine, Richmond, VA, USA [4]Department of Medicine, University of Maryland School of Medicine, Baltimore, MD, USA [5]Section of Hematology/Oncology, Department of Medicine, and Committee on Clinical Pharmacology and Pharmacogenomics, University of Chicago Medicine and Biological Sciences, Chicago, IL, USA [6]Inova Center for Personalized Health, Inova Schar Cancer Institute, Falls Church, VA, USA [7]Center for Clinical and Translational Research, Virginia Commonwealth University School of Medicine, Richmond, VA, USA [8]Charité — Universitätsmedizin Berlin, Department of Infectious Diseases and Respiratory Medicine, Berlin, Germany [9]German Center for Lung Research (DZL), Berlin, Germany [10]Biocellvia, Marseille, France [11]Pauley Heart Center, Division of Cardiology, Department of Internal Medicine, Virginia Commonwealth University School of Medicine, Richmond, VA, USA [12]Geriatrics Research and Education Clinical Center, Baltimore Veterans Administration Medical Center, Baltimore, MD, USA

*Corresponding author. 1101 East Marshall Street, Richmond, VA, 23298, USA. E-mail: francesco.celi@vcuhealth.org (F.S. Celi).

Received August 6, 2022 • Accepted August 26, 2022 • Available online 30 August 2022

https://doi.org/10.1016/j.molmet.2022.101588

mice showed augmented capillarization and elevated pro-angiogenic factors including Vegfa and its receptor (Vegfr2), the Notch ligand Jagged-1 (Jag1), and Angiopoietin-2 (ANGPT2 or ANG2) [14]. Collectively, these data indicate the importance of pro-angiogenesis factors from adipose tissue in whole body metabolism regulation, and a sex dysmorphic response to calorie overload.

In this study, we identified an unrecognized role for ANG2 as an important regulator in thermogenic fat recruitment and function, especially in females. Moreover, we present clinical observations that support the role of ANG2 in humans, particularly in females, consistent with our mechanistic observations. Collectively, our findings demonstrate the role of ANG2 in modulating energy metabolism in a sex-specific manner through the recruitment and activation of thermogenic fat.

2. MATERIALS AND METHODS

2.1. Animals

ANG2 flox/flox mice was provided by Dr. Martin Witzenrath from Charité — Universitätsmedizin Berlin. Adiponectin-Cre mice were purchased from Jackson Laboratory (Jackson Labs, Bar Harbor, ME). To evaluate whether ANG2 from the adipose tissue affects whole-body metabolism, we first created an ANG2 adipose tissue specific knockout mice model (ANG2 aKO) by cross breeding the ANG2 flox/flox to Adiponectin-Cre mice. All mice are housed under controlled temperature (22 °C) 12-hour light (06:00—17:59) to 12-hour dark (18:00—05:59) cycles at Animal Care Facility at Virginia Commonwealth University. For all experiments, male and female mice aged 8-weeks were used for long term HFD (45 kcal% fat, D12451i, Research Diets) feeding.

2.2. Indirect calorimetry

Before the metabolic phenotype measurement, mice were acclimated in metabolic chambers (PhenoMaster, TSE Systems, Inc, Germany) for 2 days. VO2, VCO2, energy expenditure (EE), respiratory exchange ratio (RER), locomotor activity (beam breaks; X + Y planes), food consumption and water intake were then measured for 5 consecutive days. EE differences between genotypes were analyzed by analysis of covariance (ANCOVA) according to the guidelines of the National Mouse Metabolic Phenotyping Center [15].

2.3. Body composition analysis

Body composition was assessed using the time-domain NMR minispec (LF90II, Bruker Optik). Briefly, mice were weighed and placed in the LF90II using a movement restrainer to allow proper measurements. Data for fat and lean mass were extracted for further analysis.

2.4. Oral glucose tolerance test (OGTT) and Intraperitoneal Insulin Tolerance Test (IPITT)

OGTT: Mice were fasted for 6 h followed by gavage feeding with D-glucose (2 g/kg) (Sigma Aldrich). Blood was then collected from the tail vein at 0, 15, 30, 60, 90, and 120 min after administration, and glucose was measured with a glucometer (AimStrip Plus, GERMAINE Lab, INC). IPITT: Mice were fasted for 4 h before undergoing an intraperitoneal injection of insulin (1U/kg) (Sigma Aldrich). Blood was then collected from the tail vein at 0, 15, 30, 45, 60, 120 min for glucose measurement with glucometer.

2.5. Serum insulin, triglyceride and free fatty acid (FFA) measurement

Serum insulin, triglyceride and free fatty acid were measured with ultrasensitive mouse Insulin ELISA kit (Crystal Chem, #90080), triglyceride colorimetric assay kit (#10010303, Cayman Chemical) and free fatty acid quantification kit (MAK044-1KT, Sigma Aldrich) respectively according to manufacturers' instruction.

2.6. Homeostasis model assessment of insulin resistance (HOMA-IR) and adipose tissue insulin resistance index (Adipo-IR) calculation

HOMA-IR was calculated with the formula: glucose (mmol/L) × insulin (mU/L)/22.5. Adipo-IR was calculated with the formula: FFA (mmol/L) × insulin (pmol/L).

2.7. Quantitative real-time PCR (qPCR)

Total RNA was extracted using TRIzol (Thermo Fisher Scientific), and cDNA was obtained from 1 μg of RNA using the iScript cDNA Synthesis Kit (Bio-Rad). Quantitative PCR was performed using target specific primers reported in Supplementary Table 1. PCR reactions consisted of 1× PowerUp SYBR Green Master Mix (Thermo Fisher Scientific), 0.5 μM forward and reverse primers, 5—20 ng cDNA (mRNA analysis) in a total reaction volume of 10 μL. Reactions were amplified as technical duplicates or triplicates on a CFX96 real-time PCR system (Bio Rad). Data were analyzed using the CFX Maestro Software (Bio Rad) with an efficiency-corrected relative quantification ($2^{\Delta\Delta}$Cq) methodology utilizing 18S as a reference gene.

2.8. Western blot

Mouse tissues were homogenized and lysed in RIPA buffer containing protease and phosphatase inhibitors (cOmplete, EDTA-free Protease Inhibitor Cocktail, PhosSTOP; Roche). Protein lysates were separated by SDS—PAGE and dry blotted to a Polyvinylidene difluoride (PVDF) membrane and further processed using established methods. Western blot signal was visualized using enhanced chemiluminescence reagents (#7003S, Cell Signaling) according to the manufacturer's protocol for ChemiDoc MP Imaging System (Bio Rad) imaging as well as film development.

2.9. Histopathology and digital imaging analysis of hepatic steatosis

Mouse adipose tissue, pancreas, and liver paraffin-embedded sections were sliced at 5 μm and stained with hematoxylin and eosin (H.E.) in the Cancer Mouse Models Core Laboratory at Virginia Commonwealth University. Images were scanned in Vectra Polaris fully-enclosed multispectral imaging system (PerkinElmer) for further histomorphology analysis. Hepatic steatosis quantification was processed with Biocellvia software (Biocellvia, Marseille, France) and expressed as a percentage of steatosis and vesicle area. Hepatic fibrosis was identified using Sirius Red stained slides and evaluated by Biocellvia software expressed as the percentage of Sirius Red stained area among total area. We also evaluated pancreatic islet morphology changes since enhancement in pancreatic islet size is always linked with the induction of insulin resistance [16].

2.10. Adipocyte size quantification

The sizes of the adipocytes were analyzed using the ImageJ version 1.53a program (https://imagej.nih.gov/ij) with the Adiposoft version 1.16 plug-in (https://imagej.net/adiposoft). The area was calculated only in the part that completely constituted one cell and adipocyte size distribution was further analyzed in Graphpad 9.0 with frequency distribution analysis.

2.11. Immuno-staining

Slices for immunofluorescence staining were rinsed in PBST and then deparaffinized and heat retrieved at 96 °C for 30 min in citrate acid

buffer. After cooling naturally, slides were rinsed in PBST again and blocked with 5% BSA (FisherSci, BP1600) for 1 h and then incubated with primary antibodies to glucagon, 1:500 (Millipore Sigma, G2654), Insulin 1:500 (Bio Rad, 5330-0104G) overnight at 4 °C. Following washes in PBST, slides were then incubated with secondary antibodies to Goat anti-Guinea Pig IgG, Alexa Fluor 568 1:1000 (Thermo Fisher Scientific, A11075), Goat anti-Mouse IgG, Alexa Fluor 488 (Thermo Fisher Scientific, A11001) diluted in PBST containing 1% BSA for 1 h at room temperature. Slides were then washed in PBST, and then mounted with Prolong Anti-Fade mounting medium containing DAPI (Thermo Fisher Scientific).

2.12. Confocal microscopy

Pancreas slides staining with anti-Glucagon and anti-Insulin antibody were imaged on a Zeiss LSM 710 Confocal Laser Scanning Microscopy (1:500, Sigma Aldrich, G2654) and (1:500, Bio Rad 5330-0104G), respectively. Cell nuclei was stained with DAPI as described above.

2.13. Cold exposure and core body temperature measurement

For short term cold exposure experiment, female control and ANG2 aKO mice were single housed in rodent incubator (RIS33SD, Powers Scientific, Inc) at 23 °C for one day. Then incubator temperature was dropped to 18 °C and kept for 4 consecutive days as adaptation. Thereafter, all mice were exposed at 10 °C for consecutive days. Core body temperature was monitored daily during the cold exposure via mice rectal probe thermometer (OMEGA HH806AW). Whole-body thermogenesis was imagined with an infrared camera (T420, FLIR).

2.14. Stromal vascular fraction cell isolation, adipocyte differentiation and estradiol (E2) treatment

Stromal vascular fraction (SVF) cells were isolated from the inguinal fat pad of a 1-month old female C57BL/6 J mouse using collagenase D (Roche) and dispase II (Roche) digestion as described previously [17]. Adipocyte differentiation was performed as described previously [18]. During this experiment, phenol red free medium (Thermo Fisher Scientific) and charcoal stripped Fetal Bovine Serum (FBS) (Sigma Aldrich, F6765) were used in order to avoid the endogenous estrogen interference as phenol red has been reported to have estrogenic activity [19]. After 2 days of induction medium, E2 (10, 100 nM) and vehicle were used to treat both beige and white adipocyte during the entire differentiation process. Fresh maintenance medium contained E2 was replaced every other day till differentiation was completed (8 days), then the adipocytes were harvested for RNA isolation and quantitative PCR assay.

2.15. Echocardiography

Cardiac function was assessed via echocardiography at the end of diet study using the Vevo2100 imaging system (VisualSonics Inc, Toronto, Canada). Mice were anesthetized with isoflurane (1.5%, delivered at a flow rate of 1 L/min), in accordance with our animal protocol throughout the duration of the procedure The general procedure for acquiring short-axis images, estimating fractional shortening (FS) and ejection fraction (EF), measuring heart rate, and obtaining left ventricular end-systolic diameter (LVESD), left ventricular end-diastolic diameter (LVEDD), cardiac output, end-systolic (ES) volume, end-diastolic (ED) volume and stroke volume has been previously described [20]. LV fractional shortening (FS) was calculated as (LVEDD-LVESD)/LVEDD*100 and Ejection Fraction (EF) was calculated using the Teichholz formula.

2.16. Human subjects study

To corroborate in humans the sex-related findings we observed in mice, we assessed the association of sex with serum ANG2 levels in 1198 subjects from the Amish Research program. Serum ANG2 was measured in subjects who had previously participated in two community-based studies of cardiovascular health and platelet function [21,22]. Subjects were generally healthy and drug naïve; all had discontinued the use of vitamins and supplements at least one week prior to sampling collection. Serum ANG2 level was measured with the R&D Systems Human Angiopoietin-2 Quantikine Immunoassays (Minneapolis, MN). Samples were processed in triplicate according to the manufacturer's instructions (R&D Systems). To control for inter-plate and inter-batch variation, aliquots from a single time point blood draw from two volunteer subjects were run on each plate in triplicate (internal controls). Serum ANG2 levels were natural log-transformed prior to analyses to reduce skewness. Body fat mass was measured by DXA in grams, using a Hologic 4500 W (Bedford, MA, USA).

2.17. Statistical analysis

For laboratory-based experiments statistical comparisons were made using the unpaired t-test or One-way ANOVA with GraphPad Prism 9. Statistical significance was accepted at a p-value of less than 0.05. P-values are represented as $*p < 0.05$; $**p < 0.01$; $***p < 0.001$ respectively.

For the human subject study, we assessed the correlation of age with ANG2 levels in males and females separately and then whether the age-ANG correlation was moderated by sex on ANG2 using multiple regression analysis. We similarly estimated the correlation of ANG2 with two adiposity-related measurements (fat mass and BMI) and then assessed whether these correlations were moderated by sex, using multiple regression analysis with adjustment for age. These analyses were performed in SAS.

2.18. Study approval

All animal study protocols were approved by the Institutional Animal Care and Use Committee of Virginia Commonwealth University. The human study was approved by the Institutional Review Board at the University of Maryland. Written informed consent was obtained from all patients or their designated family members.

3. RESULTS

3.1. Characterization of ANG2 aKO mice

ANG2 aKO mice were generated by cross breeding the ANG2 flox/flox to Adiponectin-Cre mice, and no fertility difference was observed in ANG2 aKO mice compared with controls. ANG2 deletion driven by adiponectin-CRE resulted in loss of ANG2 transcript in isolated mature adipocyte (Figure 1A). No differences in body weight or growth curve were observed in either female or male ANG2 aKO-mice fed with regular chow diet (RCD) when compared to littermates (Figure 1B and C). In contrast, female ANG2 aKO on 6-month HFD diet had significantly greater body weight gain (Figure 1D) and fat mass expansion (Figure 1E). Furthermore, female ANG2 aKO mice showed increased myocardial dimensions on echocardiogram (Fig. S1). Interestingly, no significant body weight difference was observed in male mice (Figure 1F).

3.2. Female ANG2 aKO mice show decreased energy expenditure upon HFD challenge

To determine whether the weight gain in HFD-fed female ANG2 aKO mice was attributable to altered energy metabolism, we characterized

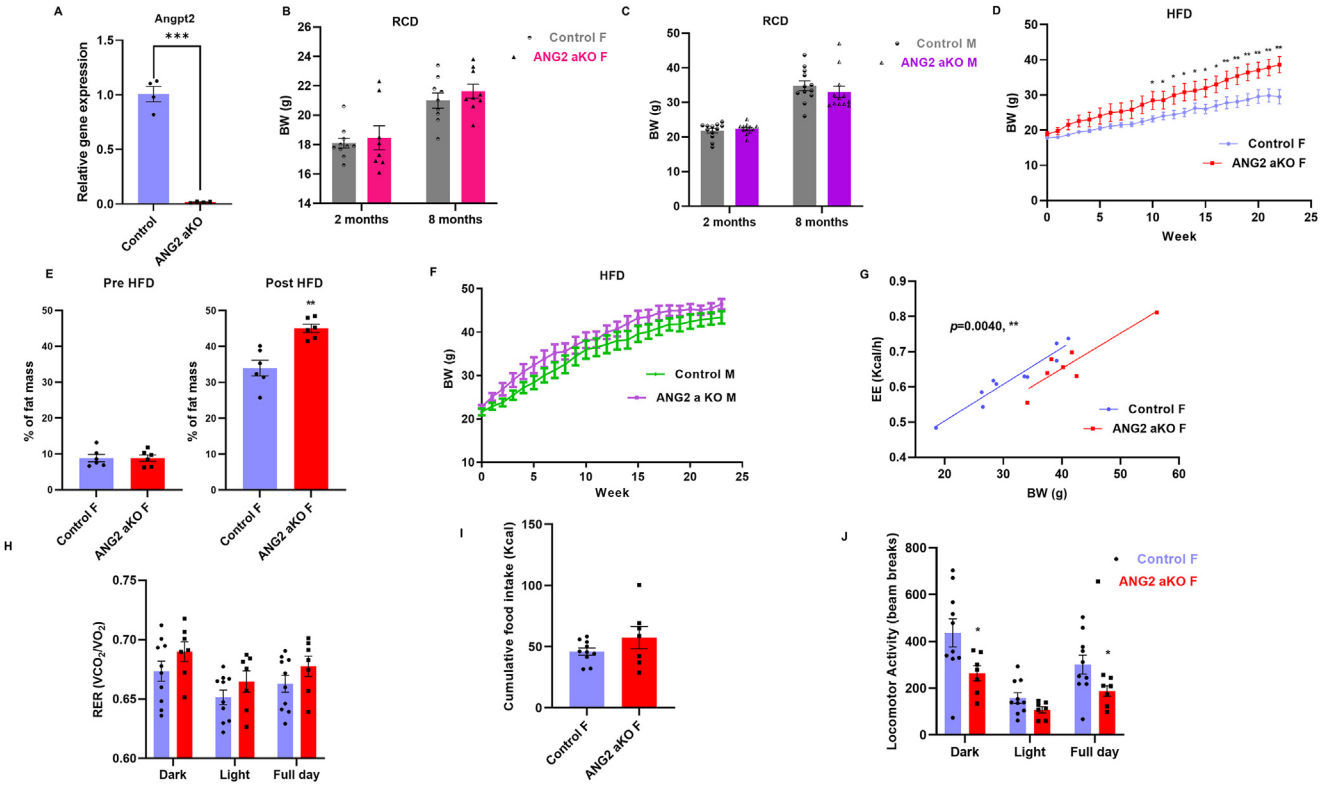

Figure 1: ANG2 deletion in female mice (ANG2 aKO) on HFD results in significant body weight gain and decreased energy expenditure. (A): Comparisons of Ang2 mRNA expression in isolated mature adipocytes in control and ANG2 aKO mice. (B): Body weight of female control and ANG2 aKO mice on RCD at 2 and 8 months. (C): Body weight of male control and ANG2 aKO mice on RCD at 2 and 8 months. (D): Body weight changes of female control and ANG2 aKO mice fed HFD. (E): Percentage of fat mass in female control and ANG2 aKO mice, before and after HFD. (F): Body weight changes of male control and ANG2 aKO mice on HFD. (G): Regression plot of full day energy expenditure, with ANCOVA analysis of energy expenditure of female control and ANG2 aKO mice on HFD (n: Control F = 10, ANG2 aKO F = 7). (H): RER in dark, light cycle and full day. (I): Cumulative food consumption reported as Kcal. (J): Locomotor activity. Data are shown as mean ± SEM $*p < 0.05$, $**p < 0.01$ vs control.

the metabolic phenotype using indirect calorimeters (PhenoMaster™). Weight-adjusted ANCOVA analysis shows that Energy Expenditure (EE) was significantly lower in HFD-fed female ANG2 aKO mice in comparison with controls (Figure 1G, Fig. S2). Respiratory Exchange Ratio (RER) was similar between groups (Figure 1H). ANG2 aKO female mice had a non-significant increase in food consumption (Figure 1I) and a significantly decreased locomotor activity (Figure 1J). Male ANG2 aKO mice on HFD did not show any significant difference in EE, RER, food consumption, or locomotor activity when compared with controls (Fig. S3). Collectively, this set of HFD-exposure experiments demonstrate that deletion of ANG2 in adipose tissue alters energy metabolism in female mice, causing obesity.

3.3. ANG2 adipocyte depletion resulted in beige fat "whitening" and adipocyte hypertrophy in perigonadal fat depot upon HFD challenge

We next investigated the effect of ANG2 adipocyte deletion on different adipose depots. ANG2 aKO female mice on HFD had larger brown fat (BAT) lipid droplets size compared with controls (Figure 2A), while the two genotypes had no significant difference in UCP1 and other lipogenesis markers such as FASN, PPARϒ, ATGL, and HSL by immunoblotting (Figure 2B and C). In mice, the subcutaneous inguinal adipose tissue depot undergoes the most profound induction of beige adipocytes in response to either cold exposure or HFD [23,24]. As expected, beige fat with a classical multilocular morphology was seen in controls, but ANG2 aKO female mice had much larger adipocytes (Figure 2D). Adipocyte distribution quantification revealed that ANG2 aKO female inguinal adipocytes were nearly triple in size when compared with controls (Figure 2E and F). Consistent with a "whitening" phenotype, browning/beige adipogenesis markers, such as Ucp1, Pgc1α, were significantly downregulated in ANG2 aKOs (Figure 2G). Immunoblotting also confirmed the downregulation of UCP1 (Figure 2H). Notably, we observed that although the protein expression of Fatty Acid Synthase (FASN) was unchanged, Adipose Triglyceride Lipase (ATGL) was significantly downregulated (Figure 2H and I). Using immunohistochemistry, we found the endothelial marker CD31 was reduced around the beige adipocyte of ANG2 aKOs compared to controls mice (Figure 2J), consistent with a decrease in vascularization. Similar to inguinal fat, histologic assessment of perigonadal fat depot showed adipocyte hypertrophy in ANG2 aKO mice (Figure 2K, L, M). Interestingly, immunoblotting showed the expression of FASN and ATGL were both significantly decreased (Figure 2N and O), suggesting decreased lipid metabolism (i.e., lipogenesis/lipolysis balance) in ANG2 aKOs. Furthermore, lipid metabolism regulators (PPARϒ, CEBPα, ADIPOQ and FABP4) were significantly downregulated, (Figure 2N and O). These results indicate that ANG2 is unlikely to be the predominant angiogenesis factor in controlling mature BAT. Conversely, the data indicate that ANG2 plays a more important role in recruitment as well as lipid homeostasis in inducible fat depots.

3.4. HFD-fed ANG2 aKO female mice have impaired carbohydrate metabolism and insulin resistance

Although no difference was observed in fasting glucose, (Figure 3A), OGTT (Figure 3B and C) and IPITT (Figure 3D and E) revealed that ANG2

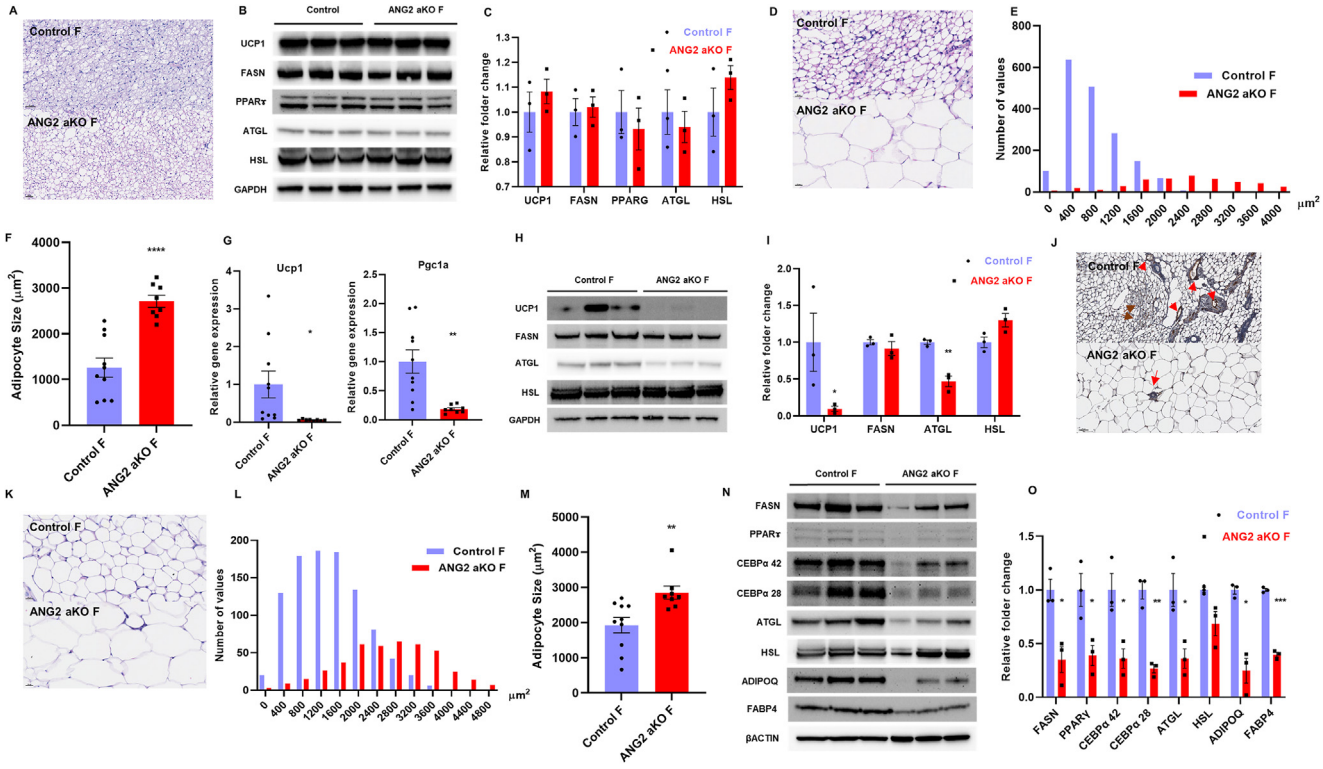

Figure 2: ANG2 adipocyte depletion resulted in beige fat "whitening" and adipocyte hypertrophy. (A): BAT sections H&E staining. Scale bars: 50 μm. (B): Immunoblots and quantification (C) of UCP1, FASN, PPARγ, ATGL, HSL and GAPDH in BAT. n = 3 each group. (D): Inguinal adipose tissue section H&E staining. Scale bars: 20 μm. (E): Adipocyte size distribution frequency and (F) quantification in both groups. (G): mRNA levels of Ucp1 and Pgc1α in inguinal fat. n = 10 each group. (H): Immunoblots and quantification (I) of UCP1, FASN, ATGL, HSL and GAPDH in inguinal fat. n = 3 each group. (J) Immunohistochemistry staining of CD31 in inguinal adipose tissue. Scale bars: 50 μm. (K): Perigonadal adipose tissue section H&E staining. Scale bars: 20 μm. (L): Adipocyte size distribution frequency and (M) quantification in both groups. (N): Immunoblots and quantification (O) of FASN, PPARγ, CEBPα, ATGL, HSL, ADIPOQ, FABP4 and βACTIN in perigonadal fat. n = 3 each group. Data are shown as mean ± SEM. $*p < 0.05$, $**p < 0.01$, $***p < 0.001$ vs Control.

aKO female mice had significant insulin resistance. Serum insulin levels and free fatty acids were also significantly elevated in ANG2 aKOs (Figure 3F and G), and consequently both HOMA-IR index and Adipo-IR index were significantly higher in ANG2 aKOs (Figure 3H and I). Moreover, H&E and immunofluorescence staining show that ANG2 aKO female mice had an expanded pancreatic islet size (Figure 3J and K). Collectively, the data indicate that ANG2 aKO female mice on HFD diet developed significant insulin resistance.

3.5. HFD feeding induced hepatic steatosis in ANG2 aKO female mice

Adiposity caused by sustained positive energy balance results in ectopic accumulation of fat in the liver [25,26], being a major contributor to the development of fibrosis (non-alcoholic steatohepatitis—NASH) and eventually cirrhosis. We thus examined whether adipose tissue-specific ANG2 ablation would result in hepatic end-organ damage. In this model, HFD did not induce changes in circulating triglycerides between genotypes (Figure 4A), while free fatty acids were increased and histology analysis demonstrated that HFD-fed ANG2 aKO female mice had significant lipid droplet accumulation in the liver (Figure 4B). Image-based quantification showed significantly increased hepatic steatosis as well as cytoplasmic vesicle areas (Figure 4C and D), but no differences in collagen scoring (Figure 4E and F). Moreover, the master lipogenic transcription factor Lxra and its associated downstream lipogenic genes, such as Cyp7a1 and Srebp1c, were both significantly downregulated in ANG2 aKO groups, while Fasn remained unchanged (Figure 4G). Consistent with the gene expression data, ANG2 aKO female mice had lower hepatic LXRα, CYP7A1, as well as SREBP1 protein expression (Figure 4H and I). These results clearly show that loss of ANG2 in AT not only affected AT function, but also caused ectopic fat deposition and consequent hepatic steatosis.

3.6. Adipose tissue-specific deletion of ANG2 results in an impaired thermogenesis in females

To determine if the metabolic phenotype changes in ANG2 aKO females were due to a defective adaptive thermogenesis response, we performed a short-term cold exposure experiment in chow-fed mice. After days of acclimation in 18 °C, mice were exposed to cold (10 °C) for 8 consecutive days. In these conditions, the core body temperature declined more drastically in ANG2 aKO mice than controls (Figure 5A ans B) before rebounding by the end of cold exposure. In another indirect calorimetry experiment, when housed at 23 °C (standard laboratory temperature but below thermoneutrality), ANG2 aKO female mice had higher EE (Figure 5C), while no significant difference was observed in body weight, food consumption, activity, or RER (Figure 5D–H). Similarly, no difference in thermogenesis-related gene expression between the genotypes was observed in brown fat (Figure 5I). Collectively, these results indicate that adipose-tissue-specific ANG2 deletion causes in females a small but physiologically relevant derangement in the adaptive thermogenesis response.

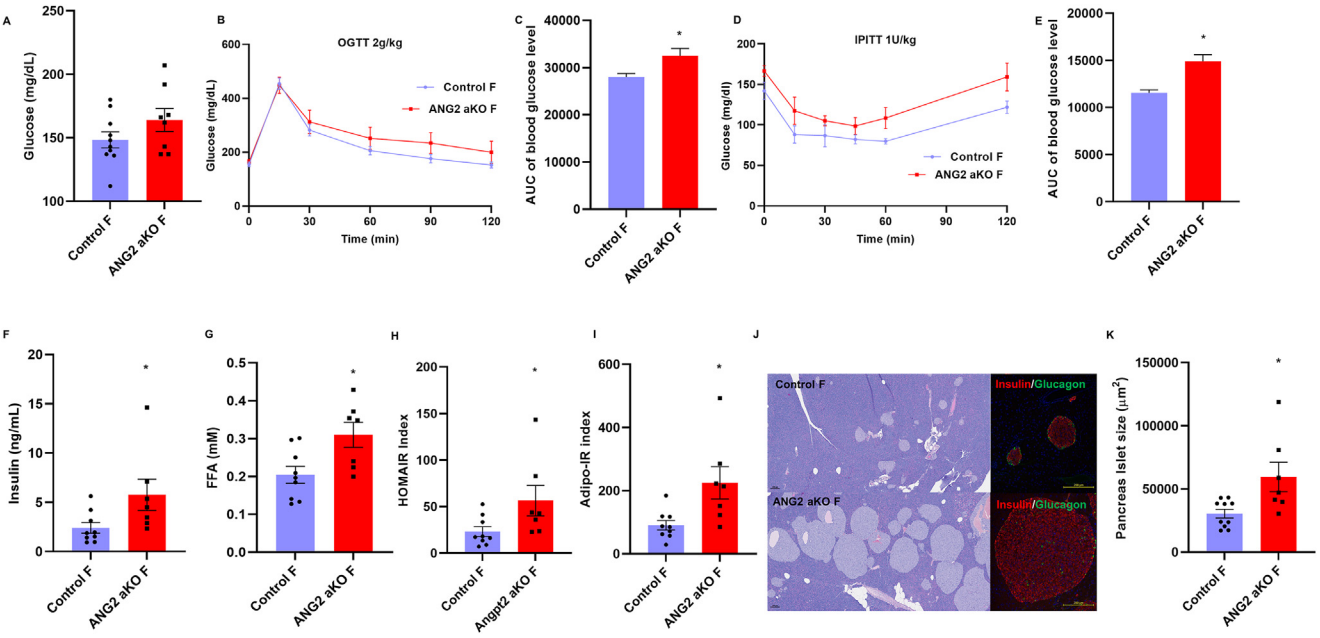

Figure 3: Female ANG2 aKO mice have impaired glucose homeostasis on HFD. (A): Fasting glucose levels measured at the end of the HFD study. (B): oral glucose tolerance test (OGTT). (C): Area under the curve from OGTT. (D): Intraperitoneal Insulin Tolerance Test (IPITT). (E): Area under the curve from IPITT. (F): Fasting serum insulin levels. (G): Fasting serum free fatty acid. (H): HOMA IR index. (I): Adipo-IR index. (J): Pancreas H&E and immunofluorescence staining insulin (red) and glucagon (green). Nuclei were stained with DAPI. Scale bars: 800 μm in H&E, 200 μm in IF staining. (K): Pancreatic islets size quantification. n ≥ 10 islets per animal. n = 10 per group. Data are shown as mean ± SEM. $^{*}p < 0.05$ vs control.

3.7. ANG2 transcript was upregulated by estradiol (E2)

The stronger association of obesity with Ang2 depletion in female compared to male mice prompted us to explore the role of estrogen in Ang2 transcription regulation in adipocytes. Preadipocytes obtained from stromovascular fraction extracted from inguinal depots of female wild-type mice were differentiated toward white or beige adipocytes (18) and exposed to E2. In white adipocytes Ang2 transcript was upregulated by 1.20 ± 0.09 fold (p = 0.34), and 1.45 ± 0.11 fold (p < 0.05), while in beige adipocytes Ang2 transcript was upregulated by 1.31 ± 0.03 fold (p = 0.14) and 1.40 ± 0.04 fold (p = 0.035) following exposure to E2, 10 nM, and 100 nM, respectively (Fig. S4B). These data support the role of estradiol in inducing Ang2 transcription in both white and beige adipocytes.

3.8. In humans circulating ANG2 is inversely correlated with body fat mass in a sex-specific manner

To evaluate the potential relevance of these findings to humans, we assessed the relationship between serum ANG2 levels and adiposity in 1,198 subjects, including how these associations might vary by sex and menopausal status. Study subjects were members of the Amish community of Lancaster, PA, aged 20–83 years who had previously participated in a community-wide cardiovascular health study as part of the Amish Research Program [21,22]. Serum ANG2 levels were natural logarithm transformed (tANG2) to remove skewness. Forty-eight percent of subjects were female, mean (SD) BMI was 26.8 ± 4.6 kg/m^2, and mean fat mass was 21.3 ± 10.2 kg (Table 1). We used linear regression models to estimate the associations of BMI and fat mass with serum ANG2 levels in males and females, and in pre- and post-menopausal females, adjusting for age. Serum ANG2 levels were higher in females than males (p < 0.001) and decreased with age in females (β = −0.005, p < 0.001), but not in males (β = 0.0009, p = 0.35) (Figure 6A). Serum ANG2 levels were significantly inversely associated with BMI, more so in females than in males (interaction p-value = 0.002) (Figure 6B). In a subgroup of subjects who underwent fat mass measurement, similar trends were also observed (Figure 6C), where ANG2 levels had more negative association with fat mass (by 4.6 unit more, p = 0.067 for the interaction effect) than male (p = 0.021).

Since ANG2 levels are regulated by estrogen level and menopause is associated with drastically reduced estrogen levels, we also investigated the association between ANG2 and menopausal status, as well as their effects on BMI and whole body fat mass in female stratified by their menopausal status. First, ANG2 levels are lower (by 0.178 unit, p = 0.152) in post-menopausal females than in pre-menopausal females, and age is negatively associated with ANG2 levels in pre-menopausal females (by 0.01 unit, p < 0.001) but not in post-menopausal females (by 0.0001 unit, p < 0.001 for the interaction effect) (Figure 6D). ANG2 levels also have negative association with BMI (Supplmentary Fig. 5A) and whole body fat mass (Supplementary Fig. 5B) in both pre- and post-menopausal females, with the effect slightly larger in pre-menopasual females. Collectively, the data support the hypothesis that in humans ANG2 plays a protective role against adiposity, in particular in premenopausal females.

4. DISCUSSION

In this study, we identified a previously unrecognized role for ANG2 as an important regulator of thermogenic fat, especially in females. Adipose tissue-selective ANG2 deletion caused reduced energy expenditure and obesity in female mice exposed to HFD. Female ANG2 adipose-deficient mice not only gained more weight than controls, but also developed metabolic traits associated with adiposity (impaired carbohydrate metabolism, ectopic fat deposition, and to a certain degree cardiovascular dysfunction). In our study population serum ANG2 was higher in females, and inversely correlated with body fat mass. These clinical observations highlight the translational relevance

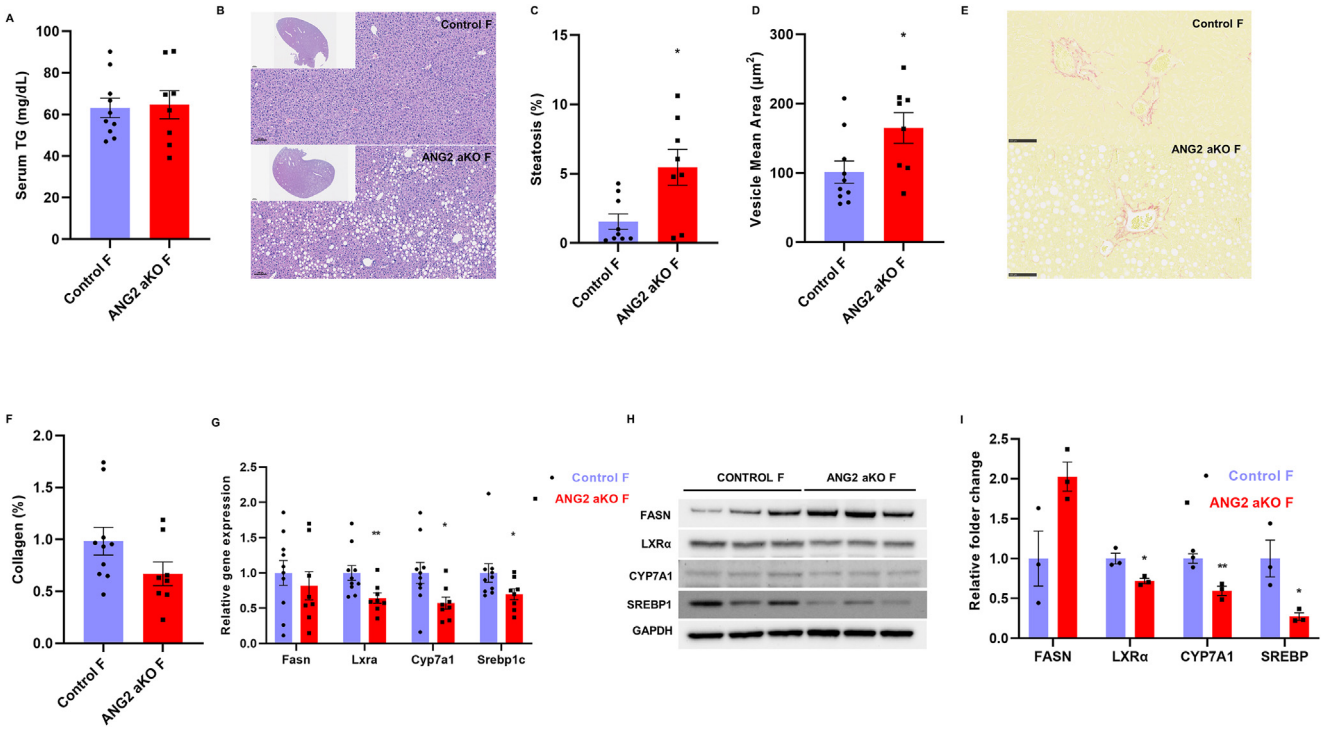

Figure 4: HFD feeding induced liver steatosis without fibrosis in ANG2 aKO female mice. (A): Serum triglyceride levels. (B): H&E staining of liver sections. Scale bars: 100 μm. (C): Percentage of steatosis quantification. (D): Vesicle area quantification. (E): Liver sections stained with picrosirius red to show collagen deposition. Scale bars:100 μm. (F): Quantification of collagen by image analysis. (G): Liver Fasn, Lxrα, Cyp7a1 and Srebp1c mRNA levels. n = 10 each group. (H): Immunoblots and quantification (I) of FASN, LXRα, CYP7A1, SREBP1 and GAPDH in liver. n = 3 each group. Data are shown as mean ± SEM. $^{*}p < 0.05$, $^{**}p < 0.01$ vs Control.

of our findings in the ANG2 KO model whereby ANG2 plays an important role in modulating energy metabolism in a sex-specific manner by mediating inducible thermogenic fat recruitment and activity.

The role of ANG2 in metabolic disorders has been previously explored. However, manipulation of ANG2 expression in adipose tissue has led to inconsistent results [27,28]. ANG2 neutralization with antibody did not show effects on body weight against HFD but resulted in impaired carbohydrate metabolism [27]. Conversely, conditional knock down of ANG2 in adipose tissue resulted in marginal weight gain and impaired thermogenic function [28]. Of note, both studies were conducted in male mice. Interestingly, in our ANG2 aKO model we did not observe differences in EE attributable to genotype when using the more rigorous ANCOVA model [29,30] to adjust body weight in male mice. Conversely, in female ANG2 aKO mice, we clearly demonstrated a difference in EE attributable to the genotype. The data demonstrate that ANG2 aKO female mice failed to recruit thermogenic fat to resist HFD-induced adiposity and developed end-organ effects of obesity. The lack of significant differences in brown adipose tissue UCP1 indicates that ANG2 is critical for beige fat recruitment but not for maintaining the activity of pre-vascularized brown fat. The delayed adaptive thermogenesis response in ANG2 aKO female mice during short-term cold exposure further confirmed its role in inducible fat recruitment. No differences in UCP-1 were observed between wild type and ANG2 aKO adipocytes derived from inguinal SVF, supporting the lack of direct action of ANG2 on adipocyte differentiation (data not shown). Interestingly, while female ANG2 aKO mice on chow diet had slightly higher EE than controls, the opposite occurred following HFD exposure at room temperature. No differences in EE were observed between HFD wild type and ANG2 aKO female mice at thermoneutrality (30°). (Fig. S6). This paradoxical finding is indeed consistent with a deficient adaptive thermogenesis response. The standard housing temperatures (20—23 °C) for laboratory mice are below the temperatures of thermoneutrality (30 °C), and at 20—23 °C, adaptive thermogenesis accounts for approximately half of their total EE to maintain the core body temperature [31,32]. Thus, when exposed to mild cold, in the absence of calorie overload and protection from heat dissipation ANG2 aKO female mice respond with activation of less energy-efficient compensatory mechanisms (muscle fasciculation, locomotor activity) driving an increase in EE. At room temperature under calorie overload, when the adaptive thermogenesis and thermogenic fat recruitment is stimulated, a defective expansion in thermogenic fat capacity due to lack of ANG2 leads to inability to dissipate the excess of calorie through thermic effect of food [33] resulting in excessive fat accumulation with the development of obesity and its metabolic consequences. Conversely, at thermoneutrality and under calorie overload, when the adaptive thermogenesis and thermogenic fat recruitment is abrogated, the effects of ANG2 on EE are abolished. In humans, impaired non-shivering thermogenesis response promotes activation of less energy-efficient muscle fasciculation, which results in the higher EE [34]. The data presented are indeed in agreement with the findings of Wolfrum and al [35]. showing only a marginal role of inguinal fat to the adaptive thermogenesis response in male mice. While our observations replicate the findings in male mice, the effects of angiopoietin-2 deletion in adipose tissue resulted in a dramatic metabolic phenotype in females. This paradoxical finding can be ascribed to the greater angiogenesis and thermogenic

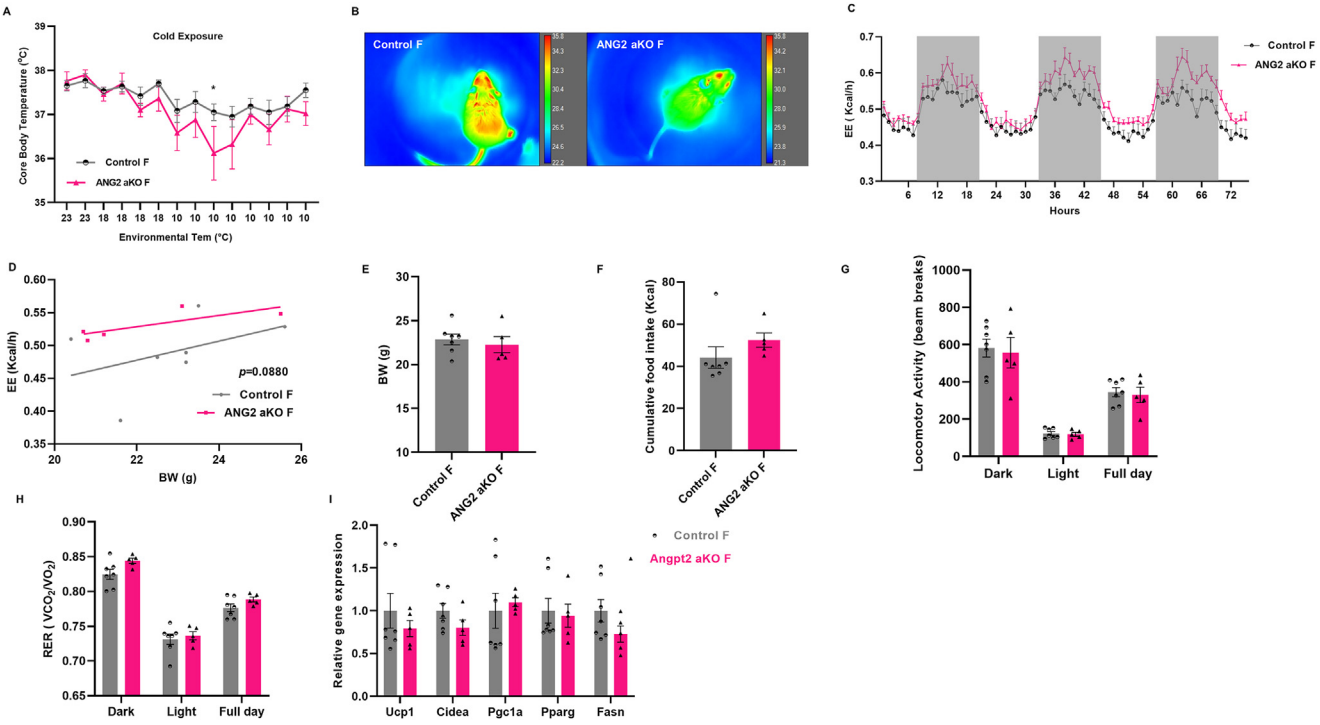

Figure 5: Chow diet-fed female ANG2 aKO mice exhibit impaired adaptive thermogenesis but slightly increased EE. (A): Changes in core body temperature during cold exposure. (B) Representative infrared thermal images of mice after three-day exposure at of 10 °C. n = 6 each group. (C): Energy expendure of chow diet-fed Control and ANG2 aKO female mice. (n: Control F = 6, ANG2 aKO F = 5). (D): Regression plot and ANCOVA analysis of full day energy expenditure in both groups. (E): Body weight. (F): Cumulative food consumption reported as Kcal. (G): Locomotor activity. (H): RER in dark, light cycle and full day. (I): BAT thermogenesis-related genes mRNA level. n = 4 each group. Data are shown as mean ± SEM. *p < 0.05 vs Control.

fat expansion in female compared to male mice when challenged with high-fat diet [14] indicating an important role of inducible fat in females, compared to male mice.

We recognize that this interpretation is speculative, and additional mechanistic studies are necessary to validate it.

The remarkable phenotypical differences between sexes in ANG2 aKO mice and the findings in the clinical study suggest the presence of an adipose estrogen-ANG2 axis that modulates whole-body metabolism. In previous studies we demonstrated that in young healthy volunteers, females had greater non-shivering adaptive thermogenesis response than males due to diffuse activation of thermogenic fat [36]. Indeed, the connection between estrogen and ANG2 has been observed in different experimental models. Ye et al. showed that estrogen therapy produced a significant Ang2 mRNA increase in heart, kidney, and lung, respectively [37], while a decreased Ang2 expression was observed in ovariectomized mice [38]. These findings support our hypothesis that ANG2 can serve as a target for mediating estrogen-regulated metabolic disorders. Weight gain in females correlates with aging and becomes more prevalent at menopause [39,40], when there is a significant loss in ovarian hormone production [41]. Moreover, the metabolic consequences of weight gain (metabolic syndrome, insulin resistance, and increase in cardiovascular risk) rise dramatically post menopause [42]. Energy expenditure studies demonstrated that, compared to pre-menopause, postmenopausal females have approximately 8% lower 24-hour resting EE [43]. This minor change can indeed have significant metabolic consequences [44]. The mechanistic effects of estrogen on energy metabolism have not been completely elucidated [45]. While estrogen replacement therapy results in lowering visceral adipose tissue, fasting serum glucose, and insulin levels [46,47], the association with increased cardiovascular disease and breast cancer risk prevents the wide use of this intervention [48–50]. Targeted activation of ANG2 might overcome this shortcoming. Further mechanistic and clinical studies will be necessary to elucidate the clinical relevance of these novel findings and to translate into interventions directed to promote expansion and activation of thermogenic fat by exploiting the estrogen-ANG2-adipose tissue axis.

Table 1 — Characteristics of study subjects according to sex.

	Total (n = 1198)	Females (n = 578)	Males (n = 620)
Age (years)			
Mean (SD)	43.5 ± 13.8	45.1 ± 14.1	42.1 ± 13.3
Median [Min, Max]	43.0 [20, 83]	45.0 [20, 83]	41.0 [20, 77]
BMI (kg/m^2)			
Mean (SD)	26.8 ± 4.6	28.0 ± 5.5	25.7 ± 3.4
Median [Min, Max]	26.1 [16.7,46.8]	27.5 [16.7, 46.8]	25.4 [18.3, 42.3]
Fat Mass (kg)			
Mean (SD)	21.3 ± 10.2	26.4 ± 9.4	15.2 ± 7.2
Median [Min Max]	20.4 [4.1,50.0]	25.9 [5.7, 50.0]	14.3 [4.1, 43.2]
Missing[a]	795	359	436
Ang-2 (pg/mL)			
Mean (SD)	1999 ± 904	2369 ± 1040	1655 ± 570
Median [Min Max]	1792.1 [688.8, 8807.0]	2144.7 [796.2, 8807.0]	1569 [688.8, 6322.4]

[a] Due to the cost of DEXA body composition analysis, not all subjects were measured for the whole body fat mass.

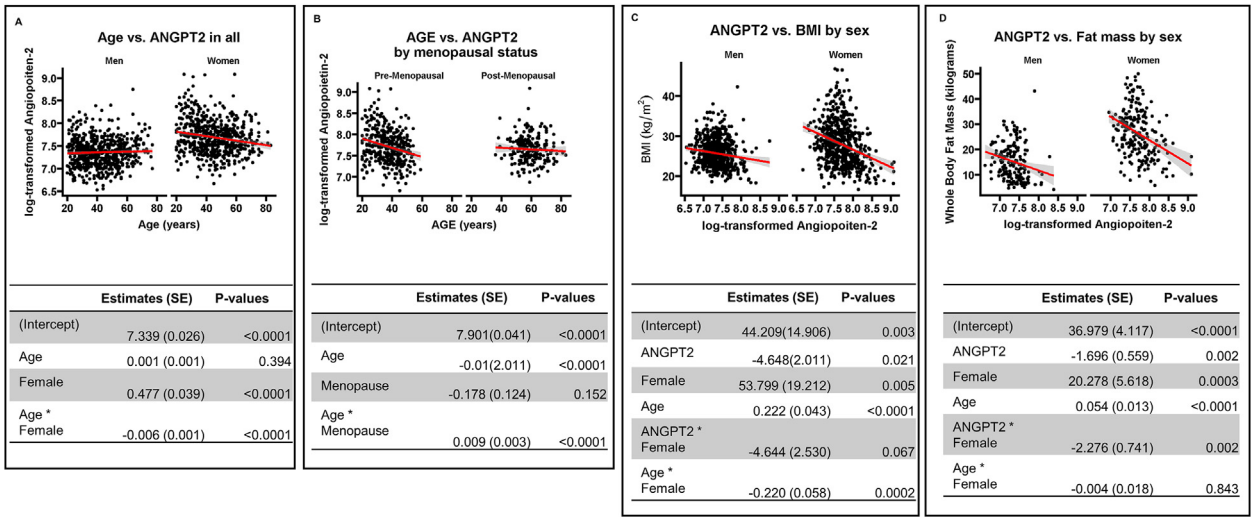

	Estimates (SE)	P-values
(Intercept)	7.339 (0.026)	<0.0001
Age	0.001 (0.001)	0.394
Female	0.477 (0.039)	<0.0001
Age * Female	-0.006 (0.001)	<0.0001

	Estimates (SE)	P-values
(Intercept)	7.901(0.041)	<0.0001
Age	-0.01(2.011)	<0.0001
Menopause	-0.178 (0.124)	0.152
Age * Menopause	0.009 (0.003)	<0.0001

	Estimates (SE)	P-values
(Intercept)	44.209(14.906)	0.003
ANGPT2	-4.648(2.011)	0.021
Female	53.799 (19.212)	0.005
Age	0.222 (0.043)	<0.0001
ANGPT2 * Female	-4.644 (2.530)	0.067
Age * Female	-0.220 (0.058)	0.0002

	Estimates (SE)	P-values
(Intercept)	36.979 (4.117)	<0.0001
ANGPT2	-1.696 (0.559)	0.002
Female	20.278 (5.618)	0.0003
Age	0.054 (0.013)	<0.0001
ANGPT2 * Female	-2.276 (0.741)	0.002
Age * Female	-0.004 (0.018)	0.843

Figure 6: Relationships between age, tANG2 (log-transformed Angiopoiten-2 levels), menopausal, and adiposity in humans. Figures show unadjusted regression results in various groups, tables under figures show results from multiple linear regression models. (A): Effect of age on tANG2 levels in males and females. Age*Female captures the differences in changes with respect to age between males and female (B): Effect of tANG2 on BMI in both sexes, adjusting for age, sex and the interaction effect of the two. ANG2*female captures the differences in the effect of ANG2 on BMI between males and females. (C): Effect of tANG2 on fat mass in both sexes, adjusting for age, sex and the interaction effect of the two. ANG2*female captures the differences in the effect of ANG2 on fat mass between males and females. (D): Effect of age on tANG2 in pre- and post-menopausal females. Age*menopausal captures the difference in changes with respect to age pre- and post-menopause.

5. CONCLUSIONS

The results of our study provided four novel findings:

1) Estrogen-ANG2-adipose tissue axis is an important and previously unrecognized determinant of adaptive thermogenesis and whole-body metabolism in mice and humans.
2) Modulation of angiogenesis plays a critical permissive role in the expansion and activation of inducible thermogenic fat, independent of the stimulating pathway for adipose tissue browning.
3) Adipose tissue-specific ANG2 aKO mouse is a novel experimental model of female obesity and its metabolic consequences.
4) In humans, there is a differential sex-driven interaction between ANG2 levels, age, and adiposity.

AUTHOR CONTRIBUTIONS

B.N. — performed the experiments, data analysis, and generation of figures and tables; involved in the conception and construction of the study; and did manuscript writing and editing.
S.S.C. — performed the human study data analysis and generation of of figures and tables; manuscript writing and editing.
K.A.R. — performed the human study data analysis and generation of of figures and tables; manuscript writing and editing.
M.L.M. — performed the human serum ANGPT2 assay and data analysis.
J.S.F. — designed and performed the Angpt2 aKO mice high resolution melting PCR genotyping.
M.W. — provided key materials for the in vivo investigations, and performed manuscript editing.
B.G. — provided key materials for the in vivo investigations.
C.S. — performed digital imaging analysis of hepatic steatosis, data analysis and manuscript editing.
K.B. — performed digital imaging analysis of hepatic steatosis and data analysis.
R.W. — performed the echocardiography and data analysis.
F.N.S. — performed the echo data analysis, provided key insights and manuscript editing.
L.M. — performed and helped the sample collection.
B.D.M. — provided key materials for clinical investigation and funding support, general guidance throughout study, and key insights and performed manuscript editing.
F.S.C. — performed data analysis, involved in the conception and construction of the study, provided critical review of the manuscript, provided guidance and mentorship throughout the study, and did manuscript writing.

DATA AVAILABILITY

Data will be made available on request.

ACKNOWLEDGMENTS

This work was funded by pilot research grant, Department of Internal Medicine, Virginia Commonwealth University. ANG2 flox/flox mice generation was co-funded by German Federal Ministry of Education and Research, Germany (BMBF) grants to M.W. in the framework of e:Med CAPSyS (01ZX1604B), PROVID (01KI20160A), e:Med SYMPATH (01ZX1906A), NUM-NAPKON (01KX2021) and MAPVAP (16GW0247), and by the German Research Foundation (DFG) grants to M.W. (SFB-TR84 C06 and C09, SFB1449 B02). The human studies were supported in part from NIH grants U01 HL072515, R01 AG18728, and U01 GM074518.

CONFLICT OF INTEREST

The authors declare that they have no known competing financial interests or personal relationships that could have appeared to influence the work reported in this paper.

APPENDIX A. SUPPLEMENTARY DATA

Supplementary data to this article can be found online at https://doi.org/10.1016/j.molmet.2022.101588.

REFERENCES

[1] Feldmann, H.M., Golozoubova, V., Cannon, B., Nedergaard, J., 2009. UCP1 ablation induces obesity and abolishes diet-induced thermogenesis in mice exempt from thermal stress by living at thermoneutrality. Cell Metabolism 9(2): 203–209.

[2] Celi, F.S., 2009. Brown adipose tissue–when it pays to be inefficient. New England Journal of Medicine 360(15):1553–1556.

[3] Hibi, M., Oishi, S., Matsushita, M., Yoneshiro, T., Yamaguchi, T., Usui, C., et al., 2016. Brown adipose tissue is involved in diet-induced thermogenesis and whole-body fat utilization in healthy humans. International Journal of Obesity 40(11):1655–1661.

[4] Chondronikola, M., Volpi, E., Borsheim, E., Porter, C., Annamalai, P., Enerback, S., et al., 2014. Brown adipose tissue improves whole-body glucose homeostasis and insulin sensitivity in humans. Diabetes 63(12): 4089–4099.

[5] Lim, S., Hosaka, K., Nakamura, M., Cao, Y., 2016. Co-option of pre-existing vascular beds in adipose tissue controls tumor growth rates and angiogenesis. Oncotarget 7(25):38282–38291.

[6] Cao, Y.H., 2010. Adipose tissue angiogenesis as a therapeutic target for obesity and metabolic diseases. Nature Reviews Drug Discovery 9(2):107–115.

[7] Tang, W., Zeve, D., Suh, J.M., Bosnakovski, D., Kyba, M., Hammer, R.E., et al., 2008. White fat progenitor cells reside in the adipose vasculature. Science 322(5901):583–586.

[8] Herold, J., Kalucka, J., 2021. Angiogenesis in adipose tissue: the interplay between adipose and endothelial cells. Frontiers in Physiology 11.

[9] Sun, K., Kusminski, C.M., Scherer, P.E., 2011. Adipose tissue remodeling and obesity. Journal of Clinical Investigation 121(6):2094–2101.

[10] Sun, K., Wernstedt Asterholm, I., Kusminski, C.M., Bueno, A.C., Wang, Z.V., Pollard, J.W., et al., 2012. Dichotomous effects of VEGF-A on adipose tissue dysfunction. Proceedings of the National Academy of Sciences of the United States of America 109(15):5874–5879.

[11] Hwang, L.L., Wang, C.H., Li, T.L., Chang, S.D., Lin, L.C., Chen, C.P., et al., 2010. Sex differences in high-fat diet-induced obesity, metabolic alterations and learning, and synaptic plasticity deficits in mice. Obesity 18(3):463–469.

[12] Lutz, T.A., Woods, S.C., 2012. Overview of animal models of obesity. Current Protocols in Pharmacology. Chapter 5:Unit5 61.

[13] Pettersson, U.S., Walden, T.B., Carlsson, P.O., Jansson, L., Phillipson, M., 2012. Female mice are protected against high-fat diet induced metabolic syndrome and increase the regulatory T cell population in adipose tissue. PLoS One 7(9):e46057.

[14] Rudnicki, M., Abdifarkosh, G., Rezvan, O., Nwadozi, E., Roudier, E., Haas, T.L., 2018. Female mice have higher angiogenesis in perigonadal adipose tissue than males in response to high-fat diet. Frontiers in Physiology 9.

[15] MMPC National Mouse Metabolic Phenotyping Center, 2017. MMPC energy expenditure analysis page.

[16] Burke, S.J., Karlstad, M.D., Collier, J.J., 2016. Pancreatic islet responses to metabolic trauma. Shock 46(3):230–238.

[17] Kir, S., White, J.P., Kleiner, S., Kazak, L., Cohen, P., Baracos, V.E., et al., 2014. Tumour-derived PTH-related protein triggers adipose tissue browning and cancer cachexia. Nature 513(7516):100–104.

[18] Ni, B., Farrar, J.S., Chen, S., Lownik, J.C., Celi, F.S., 2018. A novel role for PTK2B in cultured beige adipocyte differentiation. Biochemical and Biophysical Research Communications 501(4):851–857.

[19] Welshons, W.V., Wolf, M.F., Murphy, C.S., Jordan, V.C., 1988. Estrogenic activity of phenol red. Molecular and Cellular Endocrinology 57(3):169–178.

[20] Valle Raleigh, J., Mauro, A.G., Devarakonda, T., Marchetti, C., He, J., Kim, E., et al., 2017. Reperfusion therapy with recombinant human relaxin-2 (Serelaxin) attenuates myocardial infarct size and NLRP3 inflammasome following ischemia/reperfusion injury via eNOS-dependent mechanism. Cardiovascular Research 113(6):609–619.

[21] Shuldiner, A.R., O'Connell, J.R., Bliden, K.P., Gandhi, A., Ryan, K., Horenstein, R.B., et al., 2009. Association of cytochrome P450 2C19 genotype with the antiplatelet effect and clinical efficacy of clopidogrel therapy. JAMA 302(8):849–857.

[22] Mitchell, B.D., McArdle, P.F., Shen, H., Rampersaud, E., Pollin, T.I., Bielak, L.F., et al., 2008. The genetic response to short-term interventions affecting cardiovascular function: rationale and design of the Heredity and Phenotype Intervention (HAPI) Heart Study. American Heart Journal 155(5):823–828.

[23] Kajimura, S., Spiegelman, B.M., Seale, P., 2015. Brown and beige fat: physiological roles beyond heat generation. Cell Metabolism 22(4):546–559.

[24] Ohno, H., Shinoda, K., Spiegelman, B.M., Kajimura, S., 2012. PPARgamma agonists induce a white-to-brown fat conversion through stabilization of PRDM16 protein. Cell Metabolism 15(3):395–404.

[25] Bhatt, H.B., Smith, R.J., 2015. Fatty liver disease in diabetes mellitus. Hepatobiliary Surgery and Nutrition 4(2):101–108.

[26] Youssef, W., McCullough, A.J., 2002. Diabetes mellitus, obesity, and hepatic steatosis. Seminars in Gastrointestinal Disease 13(1):17–30.

[27] An, Y.A., Sun, K., Joffin, N., Zhang, F., Deng, Y.F., Donze, O., et al., 2017. Angiopoietin-2 in white adipose tissue improves metabolic homeostasis through enhanced angiogenesis. Elife 6.

[28] Bae, H., Hong, K.Y., Lee, C.K., Jang, C., Lee, S.J., Choe, K., et al., 2020. Angiopoietin-2-integrin alpha5beta1 signaling enhances vascular fatty acid transport and prevents ectopic lipid-induced insulin resistance. Nature Communications 11(1):2980.

[29] Kaiyala, K.J., Morton, G.J., Leroux, B.G., Ogimoto, K., Wisse, B., Schwartz, M.W., 2010. Identification of body fat mass as a major determinant of metabolic rate in mice. Diabetes 59(7):1657–1666.

[30] Tschop, M.H., Speakman, J.R., Arch, J.R., Auwerx, J., Bruning, J.C., Chan, L., et al., 2011. A guide to analysis of mouse energy metabolism. Nature Methods 9(1):57–63.

[31] Skop, V., Guo, J., Liu, N., Xiao, C., Hall, K.D., Gavrilova, O., et al., 2020. Mouse thermoregulation: introducing the concept of the thermoneutral point. Cell Reports 31(2):107501.

[32] Bastias-Perez, M., Zagmutt, S., Soler-Vazquez, M.C., Serra, D., Mera, P., Herrero, L., 2020. Impact of adaptive thermogenesis in mice on the treatment of obesity. Cells 9(2).

[33] Saito, M., Matsushita, M., Yoneshiro, T., Okamatsu-Ogura, Y., 2020. Brown adipose tissue, diet-induced thermogenesis, and thermogenic food ingredients: from mice to men. Frontiers in Endocrinology 11:222.

[34] Lee, P., Linderman, J.D., Smith, S., Brychta, R.J., Wang, J., Idelson, C., et al., 2014. Irisin and FGF21 are cold-induced endocrine activators of brown fat function in humans. Cell Metabolism 19(2):302–309.

[35] Challa, T.D., Dapito, D.H., Kulenkampff, E., Kiehlmann, E., Moser, C., Straub, L., et al., 2020. A genetic model to study the contribution of Brown and brite adipocytes to metabolism. Cell Reports 30(10):3424–3433 e3424.

[36] Chen, K.Y., Brychta, R.J., Linderman, J.D., Smith, S., Courville, A., Dieckmann, W., et al., 2013. Brown fat activation mediates cold-induced thermogenesis in adult humans in response to a mild decrease in ambient temperature. Journal of Clinical Endocrinology and Metabolism 98(7):E1218–E1223.

[37] Ye, F., Florian, M., Magder, S.A., Hussain, S.N., 2002. Regulation of angiopoietin and Tie-2 receptor expression in non-reproductive tissues by estrogen. Steroids 67(3–4):305–310.

[38] Endo, Y., Obayashi, Y., Ono, T., Serizawa, T., Murakoshi, M., Ohyama, M., 2018. Reversal of the hair loss phenotype by modulating the estradiol-ANGPT2

axis in the mouse model of female pattern hair loss. Journal of Dermatological Science 91(1):43—51.

[39] Legato, M.J., 1997. Gender-specific aspects of obesity. International Journal of Fertility and Women's Medicine 42(3):184—197.

[40] Kelly, T., Yang, W., Chen, C.S., Reynolds, K., He, J., 2008. Global burden of obesity in 2005 and projections to 2030. International Journal of Obesity 32(9): 1431—1437.

[41] Lizcano, F., Guzman, G., 2014. Estrogen deficiency and the origin of obesity during menopause. BioMed Research International 2014:757461.

[42] Kwasniewska, M., Pikala, M., Kaczmarczyk-Chalas, K., Piwonnska, A., Tykarski, A., Kozakiewicz, K., et al., 2012. Smoking status, the menopausal transition, and metabolic syndrome in women. Menopause 19(2):194—201.

[43] Hodson, L., Harnden, K., Banerjee, R., Real, B., Marinou, K., Karpe, F., et al., 2014. Lower resting and total energy expenditure in postmenopausal compared with premenopausal women matched for abdominal obesity. Journal of Nutrition Sciences 3:e3.

[44] Celi, F.S., Brychta, R.J., Linderman, J.D., Butler, P.W., Alberobello, A.T., Smith, S., et al., 2010. Minimal changes in environmental temperature result in a significant increase in energy expenditure and changes in the hormonal homeostasis in healthy adults. European Journal of Endocrinology 163(6): 863—872.

[45] Lovejoy, J.C., Sainsbury, A., Stock Conference Working, G., 2009. Sex differences in obesity and the regulation of energy homeostasis. Obesity Reviews 10(2):154—167.

[46] Munoz, J., Derstine, A., Gower, B.A., 2002. Fat distribution and insulin sensitivity in postmenopausal women: influence of hormone replacement. Obesity Research 10(6):424—431.

[47] Gormsen, L.C., Host, C., Hjerrild, B.E., Pedersen, S.B., Nielsen, S., Christiansen, J.S., et al., 2012. Estradiol acutely inhibits whole body lipid oxidation and attenuates lipolysis in subcutaneous adipose tissue: a randomized, placebo-controlled study in postmenopausal women. European Journal of Endocrinology 167(4):543—551.

[48] Chlebowski, R.T., Manson, J.E., Anderson, G.L., Cauley, J.A., Aragaki, A.K., Stefanick, M.L., et al., 2013. Estrogen plus progestin and breast cancer incidence and mortality in the Women's Health Initiative Observational Study. Journal of the National Cancer Institute 105(8):526—535.

[49] Lobo, R.A., 2017. Hormone-replacement therapy: current thinking. Nature Reviews Endocrinology 13(4):220—231.

[50] Rossouw, J.E., Anderson, G.L., Prentice, R.L., LaCroix, A.Z., Kooperberg, C., Stefanick, M.L., et al., 2002. Risks and benefits of estrogen plus progestin in healthy postmenopausal women: principal results from the Women's Health Initiative randomized controlled trial. JAMA 288(3):321—333.

